

Intraoperative molecular imaging to identify lung adenocarcinomas

Andrew D. Newton¹, Gregory T. Kennedy¹, Jarrod D. Predina¹, Philip S. Low², Sunil Singhal¹

¹Department of Surgery, University of Pennsylvania Perelman School of Medicine, Pennsylvania, PA, USA; ²Department of Chemistry, Purdue University, West Lafayette, IN, USA

Contributions: (I) Conception and design: AD Newton, S Singhal; (II) Administrative support: None; (III) Provision of study materials or patients: PS Low, S Singhal; (IV) Collection and assembly of data: S Singhal; (V) Data analysis and interpretation: S Singhal; (VI) Manuscript writing: All authors; (VII) Final approval of manuscript: All authors.

Correspondence to: Sunil Singhal, MD. Department of Surgery, Hospital of the University of Pennsylvania, 3400 Spruce Street, 6 White, Philadelphia, PA 19104, USA. Email: Sunil.Singhal@uphs.upenn.edu.

Abstract: Intraoperative molecular imaging is a promising new technology with numerous applications in lung cancer surgery. Accurate identification of small nodules and assessment of tumor margins are two challenges in pulmonary resections for cancer, particularly with increasing use of video-assisted thoracoscopic surgery (VATS). One potential solution to these problems is intraoperative use of a fluorescent contrast agent to improve detection of cancer cells. This technology requires both a targeted fluorescent dye that will selectively accumulate in cancer cells and a specialized imaging system to detect the cells. In several studies, we have shown that intraoperative imaging with indocyanine green (ICG) can be used to accurately identify indeterminate pulmonary nodules. The use of a folate-tagged fluorescent molecule targeted to the folate receptor- α (FR α) further improves the sensitivity and specificity of detecting lung adenocarcinomas. We have demonstrated this technology can be used as an “optical biopsy” to differentiate adenocarcinoma versus other histological subtypes of pulmonary nodules. This strategy has potential applications in assessing bronchial stump margins, identifying synchronous or metachronous lesions, and rapidly assessing lymph nodes for lung adenocarcinoma.

Keywords: Intraoperative imaging; pulmonary adenocarcinoma; near-infrared fluorescence imaging; indocyanine green (ICG); folate-isothiocyanate

Submitted Aug 17, 2016. Accepted for publication Sep 09, 2016.

doi: 10.21037/jtd.2016.09.50

View this article at: <http://dx.doi.org/10.21037/jtd.2016.09.50>

The problem

In cancer surgery, a successful tumor resection involves removal of all disease—this requires negative margins on the final pathology specimen and removal of all small tumor nodules. Intraoperatively, a surgeon has only two tools, visual inspection and finger palpation, to improve the outcome of a tumor resection (1).

In lung cancer surgery, positive margins (R1 or R2 residual disease) occur in up to 20% of patients undergoing attempted curative resection (2,3). Reduced tactile sense and exposure with video-assisted thoracoscopic surgery (VATS) compared to open thoracotomy makes intraoperative identification and removal of small pulmonary nodules

increasingly challenging as the percentage of patients having minimally invasive surgery compared to open thoracotomy increases (4). In one study of patients with non-small cell lung cancer amenable to VATS who underwent open thoracotomy, 8.4% had metastatic nodules in other lung lobes that would not have been discovered by VATS (5). Others have shown that significantly more overall nodules and more malignant nodules are resected in metastasectomy by thoracotomy compared to VATS (6).

Traditional intraoperative imaging techniques to assist in intraoperative identification of small pulmonary nodules such as spiral wire localization, pulmonary ultrasound, CT guidance, and fluoroscopic guidance can be technically challenging and require *a priori* knowledge of the location of

the lesion (7-10). However, many small pulmonary nodules are not identified preoperatively; in studies of pulmonary metastasectomy, 18–20% of patients had an ipsilateral malignant nodule that was not imaged preoperatively (11,12).

The solution

One potential solution to the problems of positive margins on staple lines and identification of small pulmonary nodules is the use of intraoperative molecular imaging to improve detection of tumor cells (13,14). Intraoperative molecular imaging requires two innovations: (I) a fluorescent contrast agent that can be injected systemically and selectively accumulate in the tumor tissues (14); and (II) a camera system that can detect and quantify the agent in tumor tissues (13,15).

Intraoperative molecular imaging has several features that make it attractive as an adjunct to a surgeon's hands, eyes, and clinical decision making in assisting with a tumor resection. First, it is safe because it does not require ionizing radiation. Second, the technology is visual and does not necessitate special training or expertise. Third, intraoperative imaging is easy to understand and makes it possible to visualize large surfaces in real time without disrupting the flow of an operation (16).

Specialized fluorescent dyes

A variety of fluorescent contrast agents have been used for visualization during surgeries for both benign and malignant disease. Some agents that fluoresce within the visible light spectrum (390–700 nm) have the advantage that they can be seen without special equipment. However, their effectiveness is limited by poor tissue penetration due to tissue scatter and absorption by biomolecules such as deoxyhemoglobin, oxyhemoglobin, water, and lipid as well as tissue autofluorescence (17,18).

NIR light is invisible to the naked eye. However, when NIR light is used to excite a NIR fluorophore, NIR light is emitted at one wavelength and detected at another wavelength allowing precise localization of the fluorophore. In the NIR spectrum (700–900 nm), there is decreased scatter and blood absorption, which allows increased depth of penetration into solid organs, and decreased tissue autofluorescence, which improves discrimination between normal and fluorescent tissue to increase the signal-to-background ratio (SBR) (18,19).

Near infrared camera

Early NIR camera systems designed for large animal studies served as prototypes for the FLARE™ imaging system. The FLARE™ system was first used clinically for sentinel lymph node mapping with methylene blue or indocyanine green (ICG) in women with breast cancer (19-21). This system consists of a cart with control electronics, a computer, a cooling system, an articulating arm, and an imaging head containing a custom high power light emitting diode (LED) light source, 700 nm (emission wavelength of methylene blue) and 800 nm (emission wavelength of ICG) NIR cameras, a white light color video camera, and custom optics. The NIR cameras and the white light camera acquire their images simultaneously and can be displayed as either separate images or simultaneously as an overlay (19). It is important to filter white light in the 400–650 nm range in order to get optimal NIR images (18).

Many commercial grade clinical intraoperative fluorescence imaging devices are now available. In addition, our group has demonstrated that a small portable interchangeable imager of fluorescence (SPIFF) can be less expensive but still effective for detecting fluorescent tumors. This system consists of an NIR charged coupling device (CCD) camera with an articulating light filter and an LED light source with an attached heat sink mounted on a small metal platform. The system is connected to a laptop with imaging software that allows control of the exposure time, gain, and image capture (22). Our previously published clinical studies have used a combination of this prototype small portable imaging system, the Artemis Fluorescent Imaging System (Quest Medical Imaging BV, Middenmeer, The Netherlands), and the FloCam (BioVision Technologies Inc., Exeter, PA, UK).

Results

All animal studies conducted at the University of Pennsylvania that are discussed in this manuscript were approved by the University's Institutional Animal Care and Use Committee. All clinical trials conducted at the University of Pennsylvania were approved by the University of Pennsylvania Institutional Review Board.

ICG imaging

The first fluorescent dye tested for intraoperative molecular imaging of lung nodules was ICG. ICG is a non-targeted NIR contrast agent with excitation and

emission wavelengths of approximately 785 and 800 nm. ICG specificity for tumors is obtained by the phenomenon of the enhanced permeability and retention (EPR) effect. ICG cannot escape the tight junctions of normal capillaries but extravasates from the leaky capillaries of tumors and becomes trapped in that tissue (23). Several groups have demonstrated in human patients that ICG can be used to detect hepatocellular carcinoma (HCC) and colorectal cancer liver metastases (24,25).

We demonstrated in pre-clinical studies in mice and canines that fluorescent NIR imaging with ICG is effective at identifying residual disease in a surgical wound that is not visible to the naked eye and that delineation of tumor margins is very precise using this technology (26). In our first experiment, an experienced independent surgeon examined the wound bed of mice status post incomplete resections of flank tumors by visual inspection and finger palpation. Mice with residual tumor identified by these methods were excluded. The remaining mice were then imaged with ICG, and 85% of residual tumors were identified. In a second experiment in mice status post partial resections of flank tumors with no residual tumor by visual inspection or finger palpation, 22 mice were closed and used as controls, while the other 22 mice underwent additional surgery with ICG guidance until the tumors were completely resected. All of the control mice developed recurrent flank tumors within 1 week while 20 out of 22 mice that had image guided surgery had no flank tumor recurrence at 1 week.

In another preclinical study, canines with spontaneously occurring sarcomas were imaged with ICG (27). The tumor fluoresced strongly in 14 out of 15 animals. In one canine, there was only weak tumor fluorescence; the final pathology of this tumor was a myxosarcoma, which was composed largely of myxomatous matrix rather than solid tumor parenchyma. After the primary sarcomas were resected, the wound beds were examined by the primary surgeon and assistant and classified as positive or negative for significant residual fluorescence. Negative fluorescence was seen in ten animals, and biopsy of the most fluorescent area of these wound beds showed no residual tumor. Five of the animals had areas with high fluorescence consistent with a positive margin, and residual tumor cells were confirmed in four out of five of these canines. Tissue from the area of fluorescence in the animal with no residual tumor showed inflammation on pathology.

In a follow up study in humans, we showed that ICG can be used for detection of pulmonary nodules (*Figure 1*) (28). In a study of 18 patients with a pulmonary nodule requiring

resection by thoracotomy, *in situ*, ICG identified 14 out of 18 primary nodules and an additional 5 sub-centimeter cancerous nodules which were not identified preoperatively. Three of the nodules not seen on preoperative imaging were in different lobes than the primary lesion. Nodules as small as 0.2 cm and as deep as 1.3 cm from the surface were identified. Two out of 18 nodules did not fluoresce *in vivo* but did fluoresce after they were bisected on the back table. Further analysis showed that lack of fluorescence was independent of size, histology, and metabolic activity. For the 14 nodules identified preoperatively that fluoresced *in vivo*, the average depth from the pleural surface was 0.41 cm while the average depth of the two nodules that fluoresced only *ex vivo* was 1.7 cm. Of the two nodules seen preoperatively that were not identified by ICG, one was a metastatic melanoma and one was a pulmonary embolus. Both of these lesions lacked epithelial cells, which support the theory of the EPR effect as the mechanism of ICG identification of lung tumors.

Another limitation we found with ICG is that it does not discriminate well between tumors and surrounding peritumoral inflammation (29). In a series of eight canines with lung tumors, five dogs had no post obstructive pneumonitis, and three dogs had large tumors with significant post-obstructive pneumonitis and venous congestion. In the five dogs with no post-obstructive pneumonitis, tumors were highly fluorescent, and there was no fluorescence within 5 mm of the edge of the tumor. In the three dogs with post-obstructive pneumonitis, on the other hand, there was no significant difference in fluorescence between the tumor edge and 5 mm from the tumor, and there was still significant fluorescence even at 10 mm from the tumor edge. In a proof of principal study in five humans with solid tumors, one patient had a large tumor with surrounding obstructed lung. The suspected margin was marked both by finger palpation and by NIR imaging. On pathology review, there were tumor cells beyond the margin marked by finger palpation while NIR imaging identified a large section of atelectatic lung that did not have tumor cells. Based on the limitations in specificity with ICG including accumulation in areas of inflammation, we sought a targeted molecular imaging agent that would specifically bind to and identify lung adenocarcinoma.

FR α targeted molecular imaging

FR α is a glycosylphosphatidylinositol (GPI)-anchored cell surface glycoprotein with high affinity for

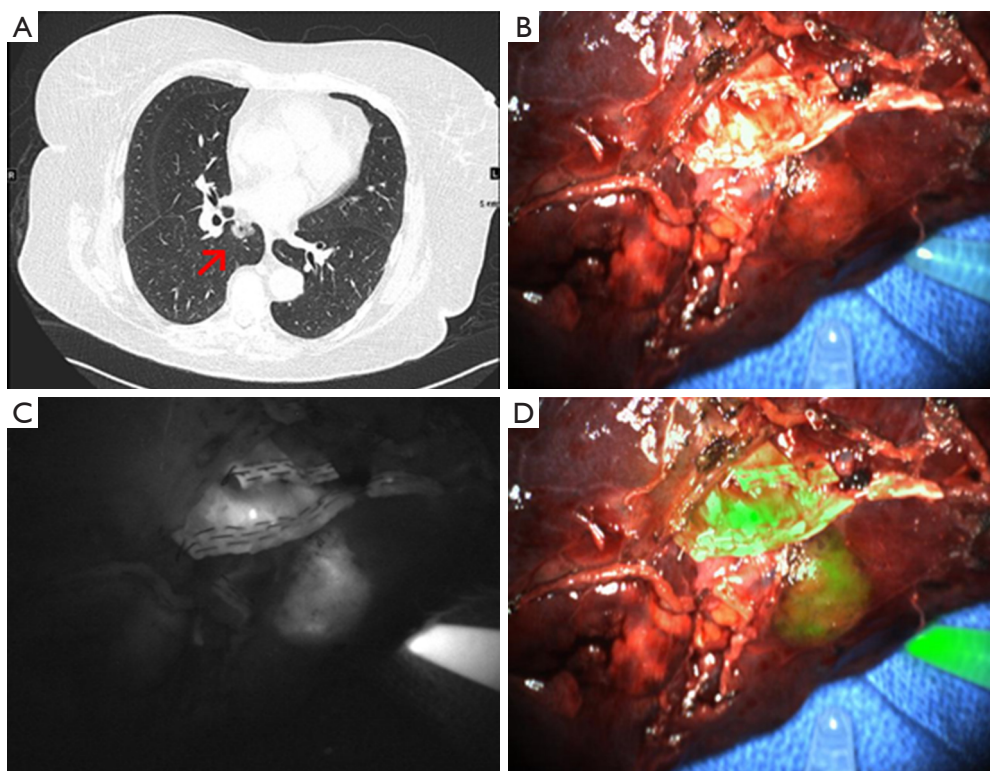


Figure 1 A representative case of ICG intraoperative imaging of a primary pulmonary adenocarcinoma. (A) Preoperative computed tomography (arrow denotes tumor); (B) *ex vivo* white light image of resected lobe; (C) near infrared image; (D) fluorescent image with overlay of white light and near infrared images. ICG, indocyanine green.

5-methyltetrahydrofolate, the primary plasma form of folate. It is part of a family of four folate receptor proteins (30). FR α is highly expressed in certain malignancies of epithelial origin (31), and expression of FR α is a positive prognostic factor in non-small cell lung cancer (32). FR α has previously been utilized as a target for folate conjugated therapies (33,34), as well as human anti-folate receptor monoclonal antibodies (35-37). Our group and others have shown that FR α is highly expressed on lung adenocarcinomas (38,39). Therefore, FR α is an appropriate target for a fluorescent tagged molecule used for intraoperative imaging of lung adenocarcinomas.

We have demonstrated that intraoperative imaging with a FR α targeted fluorescent molecular agent can be used for a variety of indications relevant to intraoperative imaging of pulmonary adenocarcinomas (Figure 2) (40). In our initial studies, we showed that intraoperative molecular imaging with a folate-fluorescein isothiocyanate (folate-FITC) conjugate (EC17), which has excitation and emission wavelengths of approximately 475 and 520 nm, correctly identified 46 out of 50 biopsy proven human lung

adenocarcinomas; the four tumors that were not identified did not express FR α . However, only 7 of the 50 tumors were seen *in vivo*, the rest were fluorescent only after they were bisected. The primary limitation of this study was poor depth of penetration by the EC17, which could be improved with a NIR fluorophore with decreased tissue scatter and blood absorption.

In a second clinical study, 30 patients with indeterminate pulmonary nodules received EC17 prior to surgery to determine the accuracy of EC17 in rapid intraoperative identification or “optical biopsy” of primary pulmonary adenocarcinomas (41). Nineteen of the 30 nodules were fluorescent. On frozen section analysis following wedge resection of these nodules, the pathologist read 13 as pulmonary adenocarcinomas, 4 as cancers of unknown origin, 1 as a squamous cell carcinoma, and 1 as containing no malignant cells. Eighteen of 19 patients underwent a lobectomy based on the frozen section analysis. However, final pathology determined that all 19 nodules were primary pulmonary adenocarcinomas: 16 invasive adenocarcinomas, 2 minimally invasive adenocarcinomas, and 1 primary

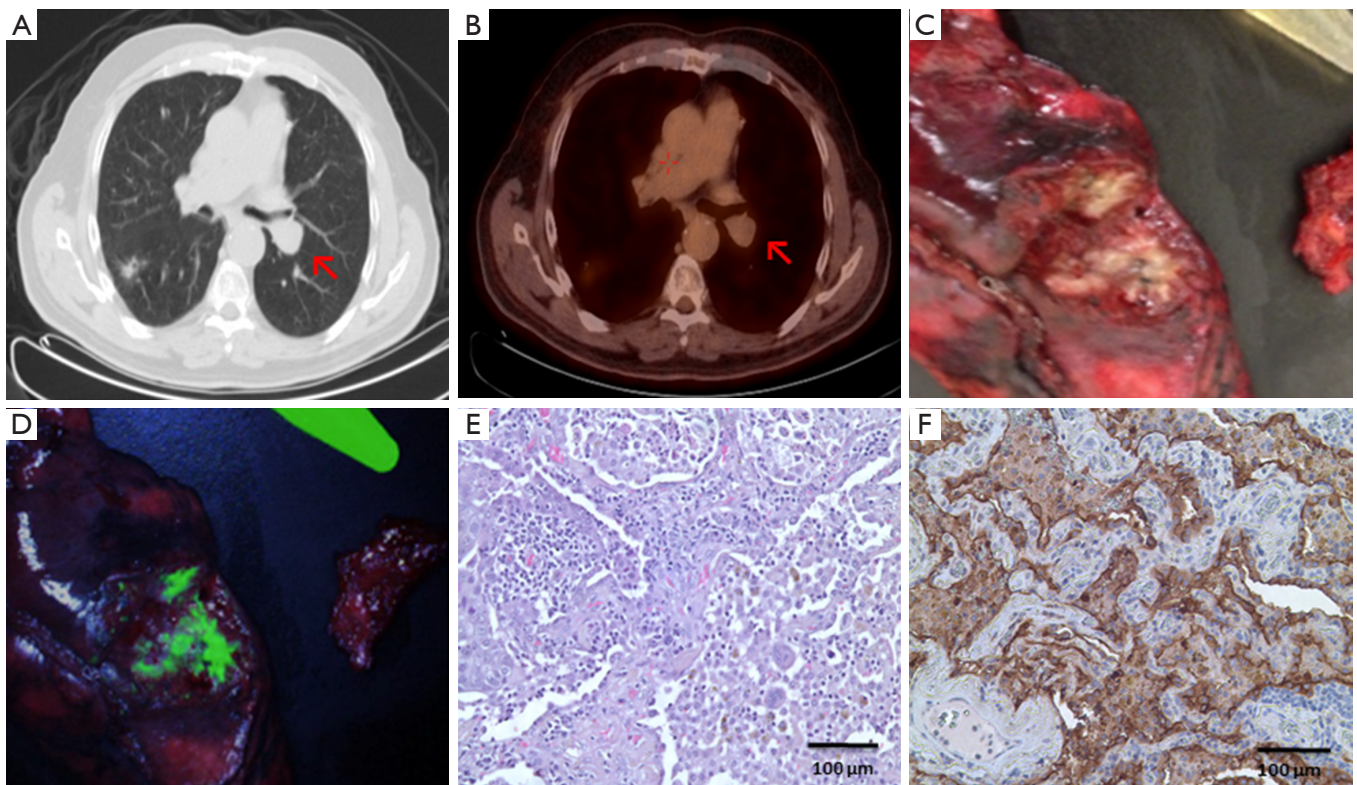


Figure 2 A representative case of folate-FITC intraoperative imaging of a primary pulmonary adenocarcinoma. (A) Preoperative computed tomography; (B) preoperative 18 fluoro-deoxyglucose positron emission tomography (arrows denote tumor); (C) bisected *ex vivo* specimen; (D) fluorescent image with FloCam imaging system; (E) hematoxylin and eosin stained frozen section; (F) folate receptor- α immunohistochemistry. FITC, fluorescein isothiocyanate.

mixed adenosquamous cell carcinoma. Importantly, the patient whose frozen section was read as benign incorrectly received a wedge resection instead of a lobectomy based on the preliminary pathologic diagnosis, when the optical biopsy was actually more accurate. Of the 11 nodules that did not fluoresce, frozen section diagnosis was benign for 5, carcinoma of unknown origin for 4, and metastatic renal cell carcinoma for 2. Final pathology showed 3 non-caseating granulomas, 2 primary squamous cell carcinomas, 2 hamartomas, 2 metastatic renal cell carcinomas, 1 metastatic leiomyosarcoma, and 1 mucocystic carcinoma. In summary, optical biopsy correctly identified 19 out of 19 primary pulmonary adenocarcinomas with no false positives or negatives. Optical biopsy took an average of 2.4 minutes compared to 26.5 minutes for standard frozen section, and it was more accurate in diagnosing lung adenocarcinomas. On further analysis, tumor histology, differentiation, size, and SUV on PET did not correlate with the degree of fluorescence.

Finally, we demonstrated that EC17 can identify additional tumor deposits at resection margins (42). In a study of mice with residual tumor intentionally left in the wound bed at resection margins, one independent investigator was able to detect residual tumor in 18 out of 60 mice with positive wound bed margins by visual inspection and finger palpation alone (30%) and falsely identified 4 mice as having positive margins. A second investigator who could utilize intraoperative imaging with EC17 in addition to visual inspection and finger palpation identified the same 18 mice with positive wound bed margins plus an additional 30 mice with residual tumors (80% accuracy total). Therefore, fluorescent imaging was 80% sensitive and 100% specific while visual inspection and manual palpation was only 30% sensitive and 90% specific for positive margins in the wound bed. It was hypothesized that the failure to detect residual tumor in some mice was due to either insufficient resolution of the camera to detect such a small area of fluorescence or poor penetration of

the tissue by EC17, which is in the visible light spectrum. A follow up series of three human patients with biopsy proven lung adenocarcinoma showed sharp demarcation between tumor and normal tissue and no residual fluorescence in the tumor bed or at the specimen margins following resection.

Summary

Intraoperative molecular imaging is a new tool with a variety of applications to the general field of surgical oncology and more specifically to lung adenocarcinomas. We have shown that a non-specific contrast agent, ICG, can accurately identify pulmonary nodules, including lung adenocarcinomas, at the time of surgery. It can detect nodules too small for detection by conventional preoperative imaging techniques, including those in other lung lobes. A folate-tagged fluorescent molecule targeted to FR α can identify pulmonary adenocarcinomas with over 90% accuracy for all pulmonary adenocarcinomas and 100% accuracy for those pulmonary adenocarcinomas expressing the FR α . We also have preliminary evidence that our imaging techniques can identify positive surgical margins, satellite metastases, and lymph nodes with cancer invasion.

Multiple clinical trials are ongoing with a FR α targeted molecule bound to a fluorophore with excitation and emission wavelengths within the NIR spectrum that should improve depth of penetration related to scatter and blood absorption while still binding specifically to FR α on lung adenocarcinomas. Other future research will involve the development of more drugs specific to other types of lung cancer. A patient ultimately could be injected with a cocktail of imaging agents that would provide a rapid intraoperative diagnosis, significantly decrease the total operative time, and allow for a more complete oncologic surgery. This technology is applicable to all solid tumors and will be increasingly utilized as new tumor specific fluorescent contrast agents are developed.

Acknowledgements

Funding: This work was partially funded by RO1 CA193556.

Footnote

Conflicts of Interest: The authors have no conflicts of interest to declare.

References

1. Aliperti LA, Predina JD, Vachani A, et al. Local and systemic recurrence is the Achilles heel of cancer surgery. *Ann Surg Oncol* 2011;18:603-7.
2. Riquet M, Achour K, Foucault C, et al. Microscopic residual disease after resection for lung cancer: a multifaceted but poor factor of prognosis. *Ann Thorac Surg* 2010;89:870-5.
3. Wind J, Smit EJ, Senan S, et al. Residual disease at the bronchial stump after curative resection for lung cancer. *Eur J Cardiothorac Surg* 2007;32:29-34.
4. Parsons AM, Detterbeck FC, Parker LA. Accuracy of helical CT in the detection of pulmonary metastases: is intraoperative palpation still necessary? *Ann Thorac Surg* 2004;78:1910-6; discussion 1916-8.
5. Cerfolio RJ, Bryant AS. Is palpation of the nonresected pulmonary lobe(s) required for patients with non-small cell lung cancer? A prospective study. *J Thorac Cardiovasc Surg* 2008;135:261-8.
6. Ellis MC, Hessman CJ, Weerasinghe R, et al. Comparison of pulmonary nodule detection rates between preoperative CT imaging and intraoperative lung palpation. *Am J Surg* 2011;201:619-22.
7. Eichfeld U, Dietrich A, Ott R, et al. Video-assisted thoracoscopic surgery for pulmonary nodules after computed tomography-guided marking with a spiral wire. *Ann Thorac Surg* 2005;79:313-6; discussion 316-7.
8. Powell TI, Jangra D, Clifton JC, et al. Peripheral lung nodules: fluoroscopically guided video-assisted thoracoscopic resection after computed tomography-guided localization using platinum microcoils. *Ann Surg* 2004;240:481-8; discussion 488-9.
9. Chella A, Lucchi M, Ambrogi MC, et al. A pilot study of the role of TC-99 radionuclide in localization of pulmonary nodular lesions for thoracoscopic resection. *Eur J Cardiothorac Surg* 2000;18:17-21.
10. Zaman M, Bilal H, Woo CY, et al. In patients undergoing video-assisted thoracoscopic surgery excision, what is the best way to locate a subcentimetre solitary pulmonary nodule in order to achieve successful excision? *Interact Cardiovasc Thorac Surg* 2012;15:266-72.
11. Cerfolio RJ, McCarty T, Bryant AS. Non-imaged pulmonary nodules discovered during thoracotomy for metastasectomy by lung palpation. *Eur J Cardiothorac Surg* 2009;35:786-91; discussion 791.
12. Cerfolio RJ, Bryant AS, McCarty TP, et al. A prospective study to determine the incidence of non-imaged

- malignant pulmonary nodules in patients who undergo metastasectomy by thoracotomy with lung palpation. *Ann Thorac Surg* 2011;91:1696-700; discussion 1700-1.
13. Singhal S, Nie S, Wang MD. Nanotechnology applications in surgical oncology. *Annu Rev Med* 2010;61:359-73.
 14. Vahrmeijer AL, Hutteman M, van der Vorst JR, et al. Image-guided cancer surgery using near-infrared fluorescence. *Nat Rev Clin Oncol* 2013;10:507-18.
 15. Mondal SB, Gao S, Zhu N, et al. Real-time fluorescence image-guided oncologic surgery. *Adv Cancer Res* 2014;124:171-211.
 16. Singhal S. The Future of Surgical Oncology: Image-Guided Cancer Surgery. *JAMA Surg* 2016;151:184-5.
 17. Jacques SL. Optical properties of biological tissues: a review. *Phys Med Biol* 2013;58:R37-61.
 18. Gioux S, Choi HS, Frangioni JV. Image-guided surgery using invisible near-infrared light: fundamentals of clinical translation. *Mol Imaging* 2010;9:237-55.
 19. Troyan SL, Kianzad V, Gibbs-Strauss SL, et al. The FLARE intraoperative near-infrared fluorescence imaging system: a first-in-human clinical trial in breast cancer sentinel lymph node mapping. *Ann Surg Oncol* 2009;16:2943-52.
 20. Ohnishi S, Lomnes SJ, Laurence RG, et al. Organic alternatives to quantum dots for intraoperative near-infrared fluorescent sentinel lymph node mapping. *Mol Imaging* 2005;4:172-81.
 21. Tanaka E, Choi HS, Fujii H, et al. Image-guided oncologic surgery using invisible light: completed pre-clinical development for sentinel lymph node mapping. *Ann Surg Oncol* 2006;13:1671-81.
 22. Okusanya OT, Madajewski B, Segal E, et al. Small portable interchangeable imager of fluorescence for fluorescence guided surgery and research. *Technol Cancer Res Treat* 2015;14:213-20.
 23. Greish K. Enhanced permeability and retention of macromolecular drugs in solid tumors: a royal gate for targeted anticancer nanomedicines. *J Drug Target* 2007;15:457-64.
 24. Ishizawa T, Fukushima N, Shibahara J, et al. Real-time identification of liver cancers by using indocyanine green fluorescent imaging. *Cancer* 2009;115:2491-504.
 25. van der Vorst JR, Schaafsma BE, Hutteman M, et al. Near-infrared fluorescence-guided resection of colorectal liver metastases. *Cancer* 2013;119:3411-8.
 26. Madajewski B, Judy BF, Mouchli A, et al. Intraoperative near-infrared imaging of surgical wounds after tumor resections can detect residual disease. *Clin Cancer Res* 2012;18:5741-51.
 27. Holt D, Parthasarathy AB, Okusanya O, et al. Intraoperative near-infrared fluorescence imaging and spectroscopy identifies residual tumor cells in wounds. *J Biomed Opt* 2015;20:76002.
 28. Okusanya OT, Holt D, Heitjan D, et al. Intraoperative near-infrared imaging can identify pulmonary nodules. *Ann Thorac Surg* 2014;98:1223-30.
 29. Holt D, Okusanya O, Judy R, et al. Intraoperative near-infrared imaging can distinguish cancer from normal tissue but not inflammation. *PLoS One* 2014;9:e103342.
 30. Elnakat H, Ratnam M. Distribution, functionality and gene regulation of folate receptor isoforms: implications in targeted therapy. *Adv Drug Deliv Rev* 2004;56:1067-84.
 31. Basal E, Eghbali-Fatourehchi GZ, Kalli KR, et al. Functional folate receptor alpha is elevated in the blood of ovarian cancer patients. *PLoS One* 2009;4:e6292.
 32. Iwakiri S, Sonobe M, Nagai S, et al. Expression status of folate receptor alpha is significantly correlated with prognosis in non-small-cell lung cancers. *Ann Surg Oncol* 2008;15:889-99.
 33. Low PS, Kularatne SA. Folate-targeted therapeutic and imaging agents for cancer. *Curr Opin Chem Biol* 2009;13:256-62.
 34. Dosio F, Milla P, Cattel L. EC-145, a folate-targeted Vinca alkaloid conjugate for the potential treatment of folate receptor-expressing cancers. *Curr Opin Investig Drugs* 2010;11:1424-33.
 35. Ebel W, Routhier EL, Foley B, et al. Preclinical evaluation of MORAb-003, a humanized monoclonal antibody antagonizing folate receptor-alpha. *Cancer Immun* 2007;7:6.
 36. Spannuth WA, Sood AK, Coleman RL. Farletuzumab in epithelial ovarian carcinoma. *Expert Opin Biol Ther* 2010;10:431-7.
 37. Konner JA, Bell-McGuinn KM, Sabbatini P, et al. Farletuzumab, a humanized monoclonal antibody against folate receptor alpha, in epithelial ovarian cancer: a phase I study. *Clin Cancer Res* 2010;16:5288-95.
 38. O'Shannessy DJ, Yu G, Smale R, et al. Folate receptor alpha expression in lung cancer: diagnostic and prognostic significance. *Oncotarget* 2012;3:414-25.
 39. Parker N, Turk MJ, Westrick E, et al. Folate receptor expression in carcinomas and normal tissues determined by a quantitative radioligand binding assay. *Anal Biochem* 2005;338:284-93.
 40. Okusanya OT, DeJesus EM, Jiang JX, et al. Intraoperative molecular imaging can identify lung adenocarcinomas

- during pulmonary resection. *J Thorac Cardiovasc Surg* 2015;150:28-35.e1.
41. Kennedy GT, Okusanya OT, Keating JJ, et al. The Optical Biopsy: A Novel Technique for Rapid Intraoperative Diagnosis of Primary Pulmonary Adenocarcinomas. *Ann*

- Surg* 2015;262:602-9.
42. Keating JJ, Okusanya OT, De Jesus E, et al. Intraoperative Molecular Imaging of Lung Adenocarcinoma Can Identify Residual Tumor Cells at the Surgical Margins. *Mol Imaging Biol* 2016;18:209-18.

Cite this article as: Newton AD, Kennedy GT, Predina JD, Low PS, Singhal S. Intraoperative molecular imaging to identify lung adenocarcinomas. *J Thorac Dis* 2016;8(Suppl 9):S697-S704. doi: 10.21037/jtd.2016.09.50